The Effects of Basal Resistance and Hydroplaning on the Initial Kinematics of Seismically Induced Tsunamigenic Landslides

Oliver-Denzil S. Taylor[1] S.M. ASCE, Aaron S. Bradshaw[2], M. ASCE, P.E., Christopher D.P. Baxter[3], M. ASCE, P.E., and Stephan T. Grilli[4], M. ASCE

[1] Graduate Student, Department of Civil and Environmental Engineering, University of Rhode Island, Kingston, RI, USA; otaylor@mail.uri.edu
[2] Assistant Professor, Department of Civil Engineering, Merrimack College, North Andover, MA, USA; bradshawa@merrimack.edu
[3] Associate Professor, Departments of Ocean / Civil and Environmental Engineering, University of Rhode Island, Narragansett, RI, USA; baxter@oce.uri.edu
[4] Professor and Chair, Department of Ocean Engineering, University of Rhode Island, Narragansett, RI, USA; grilli@oce.uri.edu

ABSTRACT: According to current landslide tsunami generation models, the initial acceleration time history of a submarine mass failure is an important factor influencing the source characteristics of tsunami waves. Translational models developed thus far typically simulate rigid or deforming bodies sliding down an inclined plane, assuming either negligible basal resistance or an idealized basal resistance, with or without the inclusion of hydrodynamic forces. However no known models incorporate realistic basal resistance, hydrodynamic forces, and hydroplaning together to quantify their effects on the initial kinematics of submarine failures. In all current models it is assumed that the maximum initial acceleration occurs nearly instantaneously after the moment of failure. Here, we propose a new rigid body model that incorporates hydrodynamic drag, with realistic basal resistance and hydroplaning effects. Utilizing the post failure shear strength of the sediment, this new model investigates the initial kinematics and time histories of the slide event in relation to tsunami generation over varying slope angles and idealized hydroplaning conditions. The current work is restricted to seismically induced submarine landslides in normally consolidated clay. The modeling results indicate a decrease in the magnitude of the peak slide acceleration by 27% to 47% and significant delays in the acceleration time histories of the sliding mass. The results also show an exponential increase in the delay of the acceleration time histories as the slope angle decreases, suggesting a greater influence of basal resistance and hydroplaning effects on typical submarine failures, for slopes of less than 5°. Further research is necessary to determine the influence of using the refined basal resistance models on predicted initial landslide tsunamis wave heights, lengths, and subsequent costal run-up elevations.

INTRODUCTION

The 1998 Papua New Guinea tsunami and the 2004 Indian Ocean tsunami, that caused the death of over 200,000 people in several countries, has focused even more the interest of various scientific communities on such geohazards. Tsunamis can be generated by volcanic eruptions, co-seismic ocean bottom motion, gas hydrate phase change, subaerial and submarine landslides, and oceanic meteorite impacts (Watts 2004). Until recently, submarine landslides have been the least studied of these tsunami generation mechanisms, mainly due to the complexity of slide failure dynamics, center of mass kinematics and landslide deformation (Locat and Lee 2002; Watts 2004). The majority of tsunamigenic submarine landslides investigated have occurred at slope angles of less than 5^o, with the most common trigger being seismic activity (Canals et al. 2004). Extreme seismic events are not required to induce tsunamigenic landslides. Frequent, moderate earthquakes can potentially trigger tsunamigenic submarine failures with resulting wave heights greater than those generated solely by the vertical displacement of the seismic ground motion (Watts 2003), thus justifying the importance of investigating seismically induced submarine failures.

Unlike subaerial landslides, submarine landslides tend to propagate for very large distances, starting as rigid blocks and then sometimes transitioning to debris flows. While research advances have been made in the past decade in the kinematics of submarine landslides, particularly in the behavior of debris flows and run-out distances, very little research has focused on the initial kinematics of these events, especially relating to tsunami generation. The transition of cohesive slides to turbidity currents, for instance, indicates that significant remolding and strength reduction can occur, which earlier research suggests, may be explained in part by the entrainment of water beneath the failed mass, causing *hydroplaning*. Recent investigations relate hydroplaning of liquefied debris flows to a critical densimetric Froude number (Fr_{crit}=0.3) that relates to a critical velocity of between 4 to 18 m/s, depending on the thickness of the failed mass (De Blasio et al. 2004 and others). In the present investigation, the critical velocity for hydroplaning to occur was taken as 6 m/s, which corresponds to Fr_{crit}=0.28, in keeping with laboratory findings. The extent to which hydroplaning occurs under the failed mass, however, is uncertain, as it depends on the rheological properties of the sediment and the geological setting of the slide, greatly complicating modeling techniques (Locat and Lee 2002).

Recent numerical modeling of tsunamigenic landslides has considered the translation (sliding) or rotation (slumping) of initially rigid bodies, moving down a plane slope with specified kinematics and deformation rate (e.g., Grilli and Watts, 2005). In such cases, results show, typical translational slides tend to produce relatively higher initial tsunami amplitudes than slumps, and a strong deformation will enhance tsunami generation, particularly in the far field. Other non-rigid slide models often assumed that the sliding mass is a liquefied debris flow from the onset of failure (e.g., Watts and Grilli, 2003). However, evidence from past failures show debris fields with large outrunner blocks where the moving sediment has remained intact giving validity to the assumption that, at least initially, the failed sediment, especially in the case of clay sediment, does not liquefy and behaves as a rigid body. Therefore,

in this study of initial kinematics, initial slide failure was modeled as and compared to other rigid body models.

A major assumption made by Grilli and Watts (2005) and others is that the influence of basal resistance is negligible on slide kinematics, as compared to the hydrodynamic drag. However, since the parameter of greatest influence on tsunami generation has been shown to be the initial acceleration of the center of the failed mass (Haugen et al. 2005; Watts et al. 2005; and others), elimination of basal resistance (i.e., soil behavior) may result in a potentially overestimated acceleration time history that is not representative of actual slide motion. Accordingly, Bradshaw et al. (2007) developed a modified solid body model, extending the work of Grilli and Watts (2005), to include effects of basal resistance on translational failures triggered by non-seismic events (i.e., rapid sedimentation and overpressures). This paper presents a further refinement of that analysis of initial slide kinematics with a model for a seismically induced slide, that accounts for effects of basal resistance, slope angle, and hydroplaning on the time history of slide acceleration.

DESCRIPTION OF SLIDE MODEL

Based on a balance of gravity, buoyancy, inertia, hydrodynamic drag and added mass, and Coulomb friction forces, Grilli and Watts (2005) expressed the center of mass motion of a rigid 2-D Gaussian-shaped body moving down an inclined plane, as (Fig. 1):

$$(\gamma + C_m)\ddot{s} = (\gamma - 1)(\sin\theta - C_n \cos\theta)g - C_d \frac{2}{\pi \cdot B}\dot{s}^2 \qquad [1]$$

where γ = ratio of the bulk density of the sediment to the density of water, θ = slope angle, g = gravitational acceleration, B = slide length (for an equivalent semi-ellipse), C_m = added mass coefficient, C_n = Coulomb friction coefficient, C_d = hydrodynamic drag coefficient, $\ddot{s}$ = slide acceleration, and $\dot{s}$ = slide velocity (the upper dots denoting time derivatives of the slide displacement [s]).

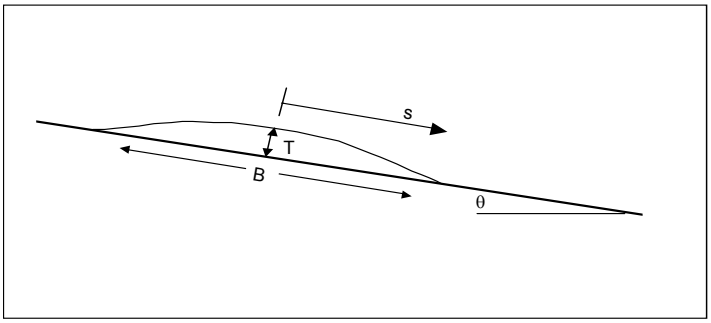

FIG. 1. Semi-elliptical rigid body utilized in modeling slide motion.

For translational failures, Grilli and Watts (2005) and Watts et al. (2005) assumed that C_n was nearly zero, once motion was initiated, thus eliminating any role of soil

behavior on the kinematics of the failed mass. Bradshaw et al. (2007) extended Eq. 1 to include basal resistance as a function of s and B:

$$(\gamma + C_m)\ddot{s} = (\gamma - 1)g \sin\theta - \frac{S(s,B)}{\rho_w \frac{\pi}{4} BT} - C_d \frac{2}{\pi \cdot B}\dot{s}^2 \quad [2]$$

where $S(s,B)$ = basal resistance function, ρ_w = density of water, and T = slide thickness.

As the focus of this study is on the initial slide kinematics, only the initial post failure conditions are considered and any deformations occurring before failure and the exact initial stress state of the slope are neglected. For a seismically induced failure, a combination of increasing pore pressures and driving stresses continue to act until the critical or yield acceleration is reached and slope instability occurs under undrained conditions. Since the duration of earthquakes is relatively short as compared to typical characteristic times of slide motion, the lateral forces induced by ground shaking (i.e., horizontal seismic accelerations) are assumed to cause failure but do not have to be considered in the post failure kinematics (Kvalstad et al. 2005).

For the nearly semi-elliptical body shown in Figure 1 the post failure motion is assumed to be initiated when the driving stress equals the peak undrained shear strength (S_u) of the clay within the weak shear zone, given by the following expression:

$$\tau_f = \rho_w \frac{\pi}{4} T \cdot (\gamma - 1) g \sin\theta = S_u \quad [3]$$

Given the results of undrained ring shear testing by Stark and Contreras (1996) on normally consolidated Drammen clay, the undrained residual shear strength (S_{ur}) is defined by the following:

$$S_{ur} = 0.55 \cdot \tau_f = 0.55 \cdot S_u \quad [4]$$

Based on Stark and Contreras's ring test results, Bradshaw et al. (2007) modeled the complete sediment strain softening behavior from peak to residual shear strength. However, given the small displacements (~ 2 cm) required to mobilize the residual strength in this sediment, it was thought that perhaps the strength behavior could be simplified to use a constant residual shear strength for all displacements. To investigate this, the present slide model was run successively with the inclusion of strain softening behavior and without. For the cases tested, no significant changes were observed in the magnitude of the peak slide acceleration and a small (0.35 s) difference occurred in the time histories. Thus, it was inferred that for these cases, strain softening at small displacements does not play a significant role in the initial acceleration time history of the slide and that the undrained residual shear strength can be assumed constant from the onset of slide movement.

In addition to residual shear strength, the other aspect considered in this study, with respect to basal resistance, is the degree of slide hydroplaning during motion. Despite

recent advances, the mechanics of slide hydroplaning are not fully understood. It is known, however, that hydroplaning can occur under varying lengths of the frontal wedge, where a water layer can become entrained, thereby decreasing the shearing resistance (De Blasio et al. 2004). Accordingly, in this study we assume, for large enough slide speeds (greater than 6 m/s here) hydroplaning occurs over a specified percentage of slide length, for which a zero basal resistance is set in the model. Note, for the hydroplaning length, we only consider the portion of the slide that overrides the sediments located down-slope from the initial failure location. Therefore, the basal resistance function, that includes soil strength and hydroplaning effects, is given by the following set of equations:

$$S(s,B) = S_{ur} \cdot (B); \qquad \{\dot{s} \le 6\,m/s \qquad [5]$$

$$S(s,B) = S_{ur} \cdot (B - s); \qquad \begin{cases} s \le B \cdot H_y \\ \dot{s} \ge 6\,m/s \end{cases} \qquad [6]$$

$$S(s,B) = S_{ur} \cdot B \cdot (1 - H_y); \qquad \begin{cases} s \ge B \cdot H_y \\ \dot{s} \ge 6\,m/s \end{cases} \qquad [7]$$

where H_y = fraction of the slide length susceptible to hydroplaning [0,1].

SENSITIVITY OF SLIDE KINEMATICS

A finite difference approach was used to solve the equation of motion (Eq. 2) utilizing the refined basal resistance (Eqs. 5-7), the undrained residual shear strength (Eqs. 3 and 4), slide properties, and varying the slope angle from 1^o to 10^o. The values modeled for the slide properties (T = 60 m, B = 4 km, and γ = 1.8) are in the typical ranges for known submarine landslides investigated in the COSTA Project (Canals et al. 2004). To analyze the effects of hydroplaning on the kinematics, H_y was varied from 25% to 100% to simulate slides that undergo partial to full hydroplaning. Coefficients C_m and C_d were taken as unity, assuming a slender and streamlined slide geometry (Grilli and Watts, 2005). These results were then compared to values obtained when assuming a zero basal resistance, as in Grilli and Watts (2005).

As could be expected, results show that as more contact exists between the slide and the sediments down slope (i.e., the smaller H_y), the greater the decrease in peak acceleration and velocity, and the effects on the time histories of slide kinematics, due to a given basal resistance (Fig. 2). Looking at Fig. 2, we see, as H_y decreases, the peak acceleration occurs earlier in the time history, but always significantly later than in the zero basal resistance model.

While Fig. 2 only shows the time histories for two slopes of 2^o and 5^o, it illustrates that as the slope angle decreases the time to peak acceleration increases for all values of H_y. The time to peak acceleration is plotted in Figure 3 over the full range of investigated slope angles (1^o to 10^o), and for the selected values of H_y. Figure 3 further indicates that for slope angles above 4^o there is no significant change in the time to peak acceleration with respect to slope angle. However, for slopes less than 4^o, the time to peak acceleration increases exponentially. This emphasizes the importance of basal resistance on slide kinematics for shallow slopes, which is critical considering

that the majority of studied tsunamigenic submarine failures occur at slope angles of less than 5^{o} (Canals et al. 2004 and others).

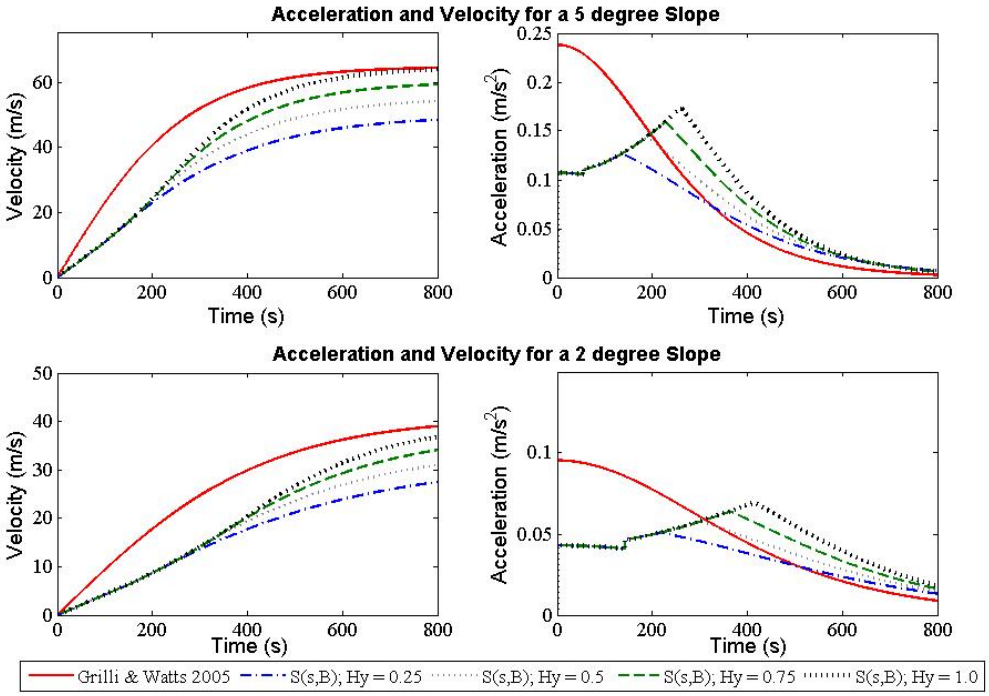

FIG. 2. Influence of hydroplaning effects for the proposed basal resistance model, at various degrees of hydroplaning H_y, on slide velocity and acceleration time histories as a function of slope (2 and 5 deg). The solid line is the zero basal resistance solution of Grilli and Watts (2005).

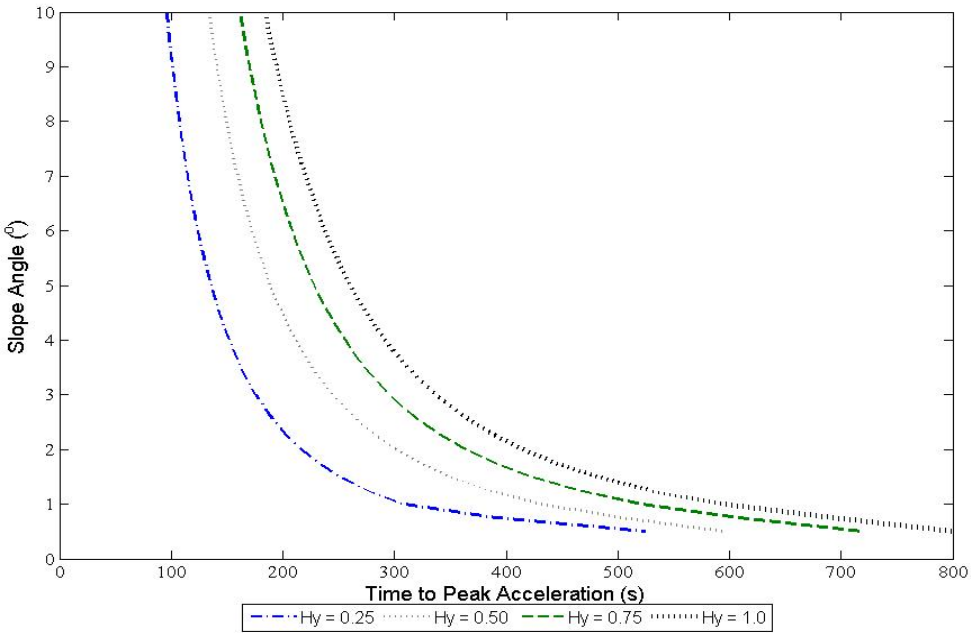

FIG. 3. Influence of failure slope angles and hydroplaning on the time to peak acceleration of the failed mass.

In addition to delaying the occurrence of the acceleration peak, Fig.2 and Table 1 show, basal resistance also significantly decreases its magnitude for all H_y cases, as compared to the zero basal resistance case. In addition, for all slope angles, reducing the portion of the slide that hydroplanes (i.e., decreasing H_y) decreases the peak acceleration. The decrease in peak acceleration, relative to the zero basal resistance case, varies from 27% for 100% hydroplaning to approximately 47% for 25% hydroplaning.

Table 1. Influence of Basal Resistance on Peak Slide Acceleration

	Peak Acceleration (m/s^2)				
Slope Angle (degrees)	**Without Basal Resistance** Grilli and Watts (2005)	**With Basal Resistance**			
		$H_y = 1.0$	$H_y = 0.75$	$H_y = 0.50$	$H_y = 0.25$
10	0.474	0.345	0.317	0.287	0.252
8	0.38	0.276	0.254	0.23	0.202
6	0.285	0.208	0.191	0.173	0.152
5	0.238	0.173	0.159	0.144	0.127
4	0.19	0.139	0.128	0.115	0.101
3	0.143	0.104	0.096	0.086	0.076
2	0.095	0.069	0.064	0.058	0.051
1	0.048	0.035	0.032	0.029	0.026

CONCLUSIONS

The results of the refined slide kinematics model reported here indicate an increasing effect of basal resistance on the initial kinematics of underwater landslides as slope angles decrease. To complicate matters, as the percentage of the slide subjected to hydroplaning decreases, the influence of basal resistance on slide kinematics also increases. In particular, the acceleration time histories are significantly affected by basal resistance, which in turn would affect tsunami generation. Based on numerical modeling, Grilli and Watts (2005) and Watts et al. (2005) show that both the magnitude and time to the peak acceleration influence the initial tsunami wave height and inundation distances. For instance, these authors report that the initial landslide tsunami maximum surface depression is roughly proportional to initial peak acceleration, which in turn similarly affects the magnitude of coastal runup. As the peak acceleration occurs later in the time history, the frontal slide wedge will also have traveled to deeper water, which will potentially further decrease the amplitude of the generated wave.

Specifically, for slopes less than 10 deg, the refined basal resistance function yields a 27% to 47% reduction in the magnitude of the peak acceleration relative to the case where basal resistance is neglected. For the mildest slopes (1 to 5 deg), which represent the majority of observed slides, the combined effects of these parameters on the initial kinematics of the failed mass would be most significant. This suggests that the assumption that basal resistance is negligible, previously made by others, may not be accurate and yield unrealistic and overestimated time histories.

These results warrant further investigations into the effects of these refined time histories on tsunami wave generation and propagation, tsunamigenic landslide case studies, and hazard assessment models. To precisely quantify the effects of the new slide kinematics derived here on tsunami amplitude and runup, new landslide tsunami generation simulations will have to be performed. This will be the object of future work.

ACKNOWLEDGMENTS

Financial support for a portion of this work was provided by a grant from FM Global, Inc. and the National Science Foundation under Grant No. 0530203. This support is greatly appreciated.

REFERENCES

Bradshaw, A.S, Baxter, C.D.P., Taylor, O-D.S., Grilli, S.T. (2007) Role of soil behavior on the initial kinematics of tsunamigenic slides. *Submarine Mass Movements and Their Consequence,s 3rd Int. Symp., Santorini, Greece* (in press).

Canals, M., Lastras, G., Urgeles, R., Casamor, J.L., Mienert, J., Cattaneo, A., De Batist, M., Haflidason, H., Imbo, Y., Laberg, J.S., Locat, J., Long, D., Longva, O., Masson, D.G., Sultan, N., and Bryn, P. (2004) Slope failure dynamics and impacts from seafloor and shallow sub-seafloor geophysical data: case studies from the COSTA project. *Marine Geology*, 213: 9-72.

De Blasio, F.V., Engvik, L., Harbitz, C.B., Elverhøi, A. (2004) Hydroplaning and submarine debris flows. *J. Geophys. Res.,* 109:C01002.

Grilli, S.T., and Watts, P. (2005) Tsunami Generation by Submarine Mass Failure. I: Modeling, Experimental Validation, and Sensitivity Analyses. *J. Waterways, Ports, Coastal, and Ocean Engng.*, 131(6): 283-297.

Haugen, K.B., Løvholt, F., and Harbitz, C.B. (2005) Fundamental mechanisms for tsunami generation by submarine mass flows in idealized geometries. *Marine and Petroleum Geology*, 22: 209-217.

Kvalstad, T.J., Nadim, F., Kaynia, A.M., Mokkelbost, K.H., Bryn, P. (2005) Soil conditions and slope stability in the Ormen Lange area. *Marine and Petroleum Geology* 22: 299-310.

Locat, J., and Lee, H. (2002) Submarine landslides: advances and challenges. *Canadian Geotechnical Journal*, 39: 193-212.

Stark, T.D., and Contreras, I.A. (1996) Constant volume ring shear apparatus. *Geotechnical Testing Journal*, 19(1): 3-11.

Watts, P., (2004) Probabilistic analysis of landslide tsunami hazards. *In: Submarine Mass Movements and their Consequences*. Locat, J., Meinert, J. (Eds.), Kluwer Academic Press, Netherlands, 1st Int. Symp. 163-170

Watts, P., and Grilli, S. T. (2003) Underwater landslide shape, motion, deformation, and tsunami generation. *Proc., 13th Offshore and Polar Engineering Conf., Intl. Soc. of Offshare and Polar Engineers*, Cupertino, Calif., 3: 364–371.

Watts, P., Grilli, S.T., Tappin, D.R., and Fryer, G.J. (2005) Tsunami Generation by Submarine Mass Failure. II: Predictive Equations and Case Studies. *J. Waterways, Ports, Coastal, and Ocean Engng*. 131(6): 298-310.